EUROPEAN ORGANIZATION FOR NUCLEAR RESEARCH

CERN–EP/90–45
CERN/LAA/MD/90–001
6 April 1990

A PRELIMINARY STUDY OF GaAs SOLID–STATE DETECTORS FOR HIGH–ENERGY PHYSICS

R. Bertin, S. D'Auria, C. del Papa, F. Fiori, B. Lisowski,
V. O'Shea, P.G. Pelfer, K. Smith and A. Zichichi

Dipartimento di Fisica dell'Università, Bologna, Italy.
Istituto Nazionale di Fisica Nucleare, Bologna, Italy.
CERN, Geneva, Switzerland.
Dipartimento di Fisica dell'Università, Firenze, Italy.
Istituto Nazionale di Fisica Nucleare, Firenze, Italy.
Dept. of Physics and Astronomy, University of Glasgow, UK.

ABSTRACT

The first phase of a study of GaAs as a base material for solid-state detectors has been completed. The main motivation behind this study is the greater radiation resistance of integrated circuits made of GaAs (compared with Si). Many diodes, of different sizes and shapes but built with the same technique, have been tested electrically and as detectors, using α–sources and minimum–ionizing particles. The tests show that these devices work with a full detection efficiency, although there is evidence for trapping of a fraction of the charge produced by the particle inside the semiconductor.

(Submitted to Nuclear Instruments and Methods in Physics Research A)

1. INTRODUCTION

The work described here has been carried out within the framework of the LAA project [1]. This project has as a goal the design of detectors that can be used at future proton colliders, where the luminosity is so high (10^{33}–10^{34} cm^{-2} s^{-1}) that the radiation resistance of the components becomes of paramount importance. For a device like the Leading Proton Detector— similar to the one being built for ZEUS at HERA [2]—the radiation resistance needed is $\sim$ 100 kGy. Silicon detectors cannot withstand such a dose, but GaAs components are harder [3]. This fact has prompted the present feasibility study.

It should be emphasized that because of the high Z (32) and density (5.32 g/cm^3), the radiation length (X_0) of GaAs is $\sim$ 2.3 cm, or four times shorter than Si. This is a disadvantage because of the greater multiple scattering, but the factor of 2 greater most probable specific energy loss (5.6 MeV/cm) implies that a 150 μm thick detector will give a signal that is equivalent to a standard 300 μm Si detector, which partially offsets the shorter X_0. Diodes of 125 μm thickness have been used in the present study. The higher forbidden band gap (1.43 eV) of GaAs (1.11 eV in Si) reduces the bulk generation current by four orders of magnitude compared with Si [4], although the energy required to create an electron-hole pair is nearly the same (4.2 and 3.6 eV, respectively) [5].

Gallium arsenide substrate material can normally be purchased with a resistivity of 10^7–10^8 $\Omega\cdot$cm, i.e. even a 500 μm thick detector is fully depleted at zero reverse bias.

2. THE DETECTORS

The GaAs basic material may be grown in a variety of ways [6,7]: MBE (molecular-beam expitaxy), LPE (liquid-phase epitaxy), VPE (vapour-phase epitaxy), HB (horizontal Bridgman), LEC (liquid-encapsulated Czochralski). *A priori*, one is naturally inclined to choose the materials known to give the best crystals (from the point of view of the transport properties): MBE, LPE, and VPE. However, MBE is only available in thicknesses of 10–20 μm owing to the too low rate of crystal growth. This thickness and the cost make MBE unsuitable for large-area detectors. Epitaxially grown material is known to provide the highest quality GaAs, but the slow rates of growth and the high cost appear to render these preparation techniques unsuitable for large-area detectors of the type required for new collider experiments. The LPE material used in early studies of GaAs detectors no longer seems to be produced commercially, and VPE is used only to a limited extent. The only manufacturer of VPE GaAs known to us (Sumitomo) can supply 2-inch diameter wafers that are almost devoid of dislocations, with nominally zero etch-pit density but unfortunately with a resistivity of only about 20 $\Omega\cdot$cm. Recent developments in the use of high growth rate, low-pressure VPE may alter this situation. It must be recalled, however, that the epitaxial layers are normally prepared on a backing of substrate material, which increases the overall thickness to typically about 500 μm. HB GaAs comes only as a low-resistivity material because of the large density of Si impurities. It therefore appears that, for the moment, only the semi-insulating LEC material is likely to satisfy the requirements for collider detectors.

The relevant characteristics of the LEC GaAs used in this study are shown in table 1.

In the standard photolithographic method that we have adopted, the wafer surface can be passivated and then etched chemically before evaporating the contacts. A thin

(10 Å) layer of oxide will normally be formed on the surface. On the other hand, it is possible to metallize the whole surface first and passivate it afterwards. Damage due to the passivation process will then be avoided underneath the contacts.

The present study has been made either using silicon dioxide (SiO_2) or with no passivation. Silicon nitride (Si_3N_4) is now the passivating material mainly used by industry. Since the thermal coefficient of SiO_2 (5.5×10^{-7} °C^{-1}) is very different from that of GaAs (6.7×10^{-6} °C^{-1}), there is a possibility of damage to the crystal. Recent studies [8] have shown that Si_3N_4 also reduces the surface leakage current by one order of magnitude compared with SiO_2, thus encouraging us to use Si_3N_4 in future tests.

The standard—albeit not unique—choice of metals for the contacts is Ti/Pt/Au for the Schottky contact and Ge:Au/Ni/Au for the ohmic one [9]. No ion implantation has been used to lower the resistivity of the material behind the ohmic contact, so as to avoid the subsequent thermal annealing. The adhesion of the metals to the semiconductor was found to be adequate.

3. TESTS

3.1 Electrical tests

We have looked at the I–V characteristic curves for a variety of diodes. A representative curve is shown in fig. 1a. The forward current rises slowly with the voltage: this does not come as a surprise, given the resistivity of the basic material (semi-insulating). The reverse current is high, varying somewhat from diode to diode, but it is roughly around 20 nA/mm^2 at -100 V, independent of the use of passivation. The general behaviour is that of a diode with well-made contacts. We probably have to understand the causes of such a high reverse current, which may be reduced using Si_3N_4 as already mentioned but may also depend on bulk generation centres, still to be identified. A C–V curve is shown in fig. 1b: the curve is flat, indicating that the diode is fully depleted even at zero bias, as expected. The value of the capacity is consistent with the expected value, taking into account the surface and the thickness of the GaAs.

3.2 Tests with sources

The calibration of the multichannel analyser is shown in fig. 2. This calibration has been checked using a Si detector and a β-source to make sure that the position of the β peak was in the expected channel. The noise performance of the set-up has also been measured. Figure 3 is a plot of the energy resolution obtained with a pulser as a function of shaping time. The best performance is obtained at 0.5 to 1 μs shaping time, depending on the leakage current. Figures 3a and 3b each correspond to a different value of the leakage current.

We have started with an α-source (^{241}Am). The $\sim$ 5.5 MeV particles stop in about 20 μm, delivering all their energy to the crystal and producing $\sim 1.3 \times 10^6$ pairs. Figure 4 shows one spectrum. The measured energy resolution is about 2%. We have observed that the position of the peak (fig. 5) moves to higher channels with bias, indicating that not all of the charge produced is collected. Beta spectra are shown in figs. 6, 7, and 8. The beta spectra have been taken using a 0.7 mm diameter plastic collimator in front of the diode and two scintillators at the back of it to open the gate of the MCA. Since the betas from ^{90}Sr have an end-point energy of 2.3 MeV, the particles we see (fig. 6) are minimum-ionizing particles (MIPs), and the spectrum

shows an essentially complete separation between pedestal and signal. This means that the partial charge collection does not affect the full detection efficiency. Spectra have also been taken for 3.5 MeV (end-point) electrons from ^{106}Ru (fig. 7): the peak of these betas overlaps with the one from ^{90}Sr, proving that we are looking at MIPs. In addition, fig. 8 shows a spectrum of betas from ^{106}Ru, with a sheet of plastic placed between the diode and the scintillator to absorb electrons with energy smaller than 2.3 MeV; again the peak of the spectrum appears in the same channel. The large number of pedestal counts is partially due to cosmic rays ($\sim$ 10 counts per minute) but mostly to geometrical inefficiency. The width of the pedestal shows that the equivalent noise charge (ENC) is 400 e. The charge collection efficiency is shown in fig. 9 for alphas and betas. It is substantially lower for MIPs owing to the different distribution of energy loss inside the semiconductor (see the Appendix). In the case of MIPs, electron-hole pairs will be produced near the back of the diode, so that if holes are trapped almost immediately, the electrons will give a smaller contribution to the charge collected than will alphas, where all the pairs are produced near the front contact. For most semiconductors, the hole trapping length is about two orders of magnitude shorter than the electron trapping length. It should be stated that beta spectra obtained with the source near the front and at the back of the diode are identical, while spectra taken with the α-source under the same conditions are very asymmetric; the alpha spectrum taken with the source near the ohmic (back) contact is reduced to a few counts with a flat distribution up to the maximum channel observed in the spectrum taken with the source on the side of the rectifying (front) contact. This proves that holes are collected with far less efficiency than electrons.

Figure 10 shows a gamma spectrum from ^{57}Co. The energy of the gammas is 122 keV, which is higher than the energy lost by a MIP ($\sim$ 70 keV). The peak of the spectrum is located in a channel that is consistent with the greater energy deposition and a charge collection almost as high as that of the alphas (see Appendix).

3.3 Beam tests

Finally, we have used a 6 GeV/c hadron beam (mainly π's) for a final check of the response of our detectors to MIPs. In fig. 11, a spectrum of energy deposited by the beam in the GaAs is shown: the diode used here has a better charge collection (47% at -100 V bias) than the one used for the tests described in the previous subsection. The peak position, for this diode, is the same for betas and for high-energy hadrons. A detection efficiency curve as a function of bias voltage is presented in fig. 12, showing that we reach $\sim$ 98% detection efficiency starting at -40 V. It should be noticed that the spectrum presented (fig. 11) shows some edge effects of the diode. This is seen as the low number of counts that joins the pedestal to the signal spectrum. The uncertainty related to these edge effects is a major contribution to the missing 2% of efficiency.

4. CONCLUSIONS

The detection efficiency is the most important point for a position-sensitive detector, and we have proved that our detection efficiency is excellent, $\sim$ 98%. The use of Si_3N_4 passivation may improve the performance substantially by reducing the noise. Making the metal contacts before passivating may also improve the state of the surface under the contacts, thus reducing the number of traps.

The GaAs diodes produced do not have an ideal performance because the charge collection is not perfect. Nevertheless, if we accept the concept that microstrips and large-surface detectors must be made with easily available material at acceptable prices and in the quantities that are needed at future colliders, then the only options appear to be to continue to work with LEC wafers and to improve the energy resolution of these diodes.

Preliminary results on radiation-hardness testing support the initial assumption that GaAs detectors are more radiation-resistant than Si ones. Detailed results of these tests will be presented in a forthcoming paper.

Acknowledgements

We would like to thank Dr L. Kelly and the staff at the National Microelectronics Research Centre, Cork, Éire, and the staff of the Dept. of Electrical and Electronic Engineering at the University of Glasgow, UK, for providing us with the diodes we have tested.

We would like to express our gratitude to the following colleagues and friends for their collaboration: Dr B. Rojas and his collaborators at SGS-Thomson (Agrate-Brianza), Professor F. Nava (University of Modena), Dr F. Vidimari (Telettra SPA), Dr A. Muchino of MASPEC (CNR–Parma), and Professor P.F. Manfredi (University of Pavia).

Table 1

Relevant properties of the GaAs as claimed by the manufacturer

Property	Value
Diameter (mm)	50.9
Orientation	(100)
Dopant	Nil
Wafer flatness (μm)	< 3
Wafer thickness (μm)	500 ± 25
Weight (g)	5.37
Resistivity ($\Omega \cdot$ cm)	7.5×10^7–1.2×10^8
Mobility (cm^2 V^{-1} s^{-1})	6.8×10^3–6.6×10^3
Carrier concentration (cm^{-3})	1.2×10^7–8.2×10^6
EPD (cm^{-2})	2.1×10^4–3.0×10^4

REFERENCES

[1] A. Zichichi, Report on the LAA Project, Vol. 1, 15 December 1986.

[2] ZEUS Collaboration, The ZEUS detector, Technical proposal, DESY–HERA, March 1986.

[3] J.M. Borrego et al., IEEE Trans. Nucl. Sci. **NS–23** (1976) 1671.
D. Harthill, IEEE Trans. Nucl. Sci. **NS–33** (1986) 36.

[4] S.M. Sze, Physics of semiconductor devices (J. Wiley & Sons, Inc., New York, 1981).

[5] M. Cuzin, Nucl. Instrum. Methods **A253** (1987) 407.

[6] J.J. Gilman, The art and science of growing crystals (J. Wiley and Sons, Inc., New York, 1963).

[7] M. Descheler et al., *in* Topical Conf. on Semiconductor Growth, Processing and Devices, Gainesville (Fla), 1984 (Univ. Florida, Gainesville, 1984) p. 187.

[8] T. Kobayashi at al., IEEE Trans. Nucl. Sci. **NS–23** (1976) 97.
J. Eberhart et al., Nucl. Instrum. Methods **94** (1974) 46.
P.E. Gibbons and J.M. Howes, IEEE Trans. Nucl. Sci. **NS–19** (1977) 353.

[9] H.K. Henisch, Semiconductor contacts (Oxford Science Publications, Oxford, 1984).
B. L. Sharma, Metal-semiconductor Schottky barrier junctions and their applications (Plenum Press Inc., New York, 1984).

[10] D.H. Lee et al., IEEE Trans. Electron Devices **ED–35** (1988) 1695.

Figure captions

Fig. 1: a) I-V curve for a diode of 8 mm^2 surface. The reverse current is $\sim$ 160 nA. The slope of the forward current is of the order of magnitude that can be calculated from the resistivity of the bulk material. b) C-V curve for the same diode as that of fig. 1a. Full depletion is demonstrated by the fact that the capacity is independent of bias.

Fig. 2: Calibration of the analog chain: preamplifier Ortec 142A, amplifier shaper Ortec 672, multichannel analyser Silena.

Fig. 3: Noise curve (obtained with a pulser) versus shaping time. At 0.5 μs, the noise has a σ of 8 channels, corresponding to 400 e using the calibration of fig. 2. The noise measured is consistent with theoretical formulas (for Gaussian shaping) using the value of the reverse current and a diode capacity of 10 pF. The amplifier gain is 200.
a) Leakage current: 160 nA.
b) Leakage current: 42 nA.

Fig. 4: Charge spectrum from an ^{241}Am α-source. The value of the peak shows that only part of the charge is collected. The HWHM on the upper part of the spectrum is about 1% of the peak. The position of the peak is a function of the bias voltage.

Fig. 5: Position of the peak of the alpha spectrum as a function of the bias voltage.

Fig. 6: Beta spectrum, taken in coincidence with a scintillator in the back of the diode. The source is ^{90}Sr. The spectrum is completely separated from the pedestal, showing that the detection efficiency is $\sim$ 100%. Bias = -100 V, amplifier gain = 200; Gaussian shaping. Shaping time = 0.5 μs.

Fig. 7: Same as fig. 6, using ^{106}Ru as the source. Despite the different electron energy, the peak is in the same channel as in fig. 6.

Fig. 8: Same as fig. 7, but a plastic absorber has been placed between the detector and the scintillator so that only high-energy ($>$ 2.3 MeV) electrons produce a trigger.

Fig. 9: Charge collection efficiency as a function of bias for alphas and betas. The result of the calculation described in the Appendix is also shown. The agreement between the measured and calculated efficiencies is reasonable.

Fig. 10: Gamma spectrum from ^{57}Co. The amplifier gain is 200 with a reverse bias of -100 V. Gaussian shaping. Shaping time = 0.5 μs. See Appendix for a comment on the charge collection efficiency.

Fig. 11: High-energy (6 GeV/c) hadron-beam spectrum. There is complete separation between noise and particle signals. Bias = -100 V, amplifier gain = 200, Gaussian shaping. Shaping time = 1 μs. Diode leakage current = 20 nA.

Fig. 12: Efficiency curve for the same diode as in fig. 11. This curve is obtained with the standard method of calculating the ratio between the hits seen in the diode and the coincidences in four external detectors covering completely the diode under test. The presence of a plateau corresponding to a detection efficiency of 95% is evident.

APPENDIX

In the case of alpha spectra, the charge collection efficiency can be calculated assuming that the electrons moving away from the junction are reduced in number from the generation point (x=0) to the collection point (x=t) with an exponential attenuation (attenuation length = λ). The holes are supposed to have a much smaller attenuation length and will not be taken into account. The contribution of dn electrons which get trapped at a distance x, to the charge collected, is given by Ramo's theorem:

$$dQ = dn\ e\ \frac{x}{t} = e\ \frac{x}{t}\ \frac{dn}{dx}\ dx = N_0\ e\ \frac{x}{t}\ P(x)\ dx\ ,$$

where N_0 is the total number of electrons produced by the alpha particle and e is the electron charge. The electrons that do not get trapped within the semiconductor give a contribution:

$$e\left(N_0 - N_0 \int_0^t P(x)\ dx\right)\ .$$

Integrating the first contribution for $0 < x < t$, adding the second contribution, and dividing out eN_0, we get the charge collection efficiency:

$$\epsilon_\alpha(\lambda) = \frac{\lambda}{t}\ (1 - e^{-t/\lambda})\ .$$

For instance, using for ϵ_α the measured number, we obtain an attenuation length of 93 μm at -100 V bias. The charge collection efficiency for betas can then be calculated integrating over the generation points of the electrons. We find

$$\epsilon_\beta(\lambda) = \frac{\lambda}{t} - \frac{\lambda}{t}\epsilon_\alpha(\gamma)\ .$$

Figure 9 shows the comparison between charge collection efficiency calculated and measured. This simple model cannot explain the ^{57}Co spectrum since it predicts a collection efficiency decreasing too slowly as a function of the electron generation point to explain the quick drop of the spectrum at the lower end. However, since λ depends on the inverse of the trapping cross-section, which in turn depends on the electric field, then λ is a function of x. A realistic model will have to take this point into account.

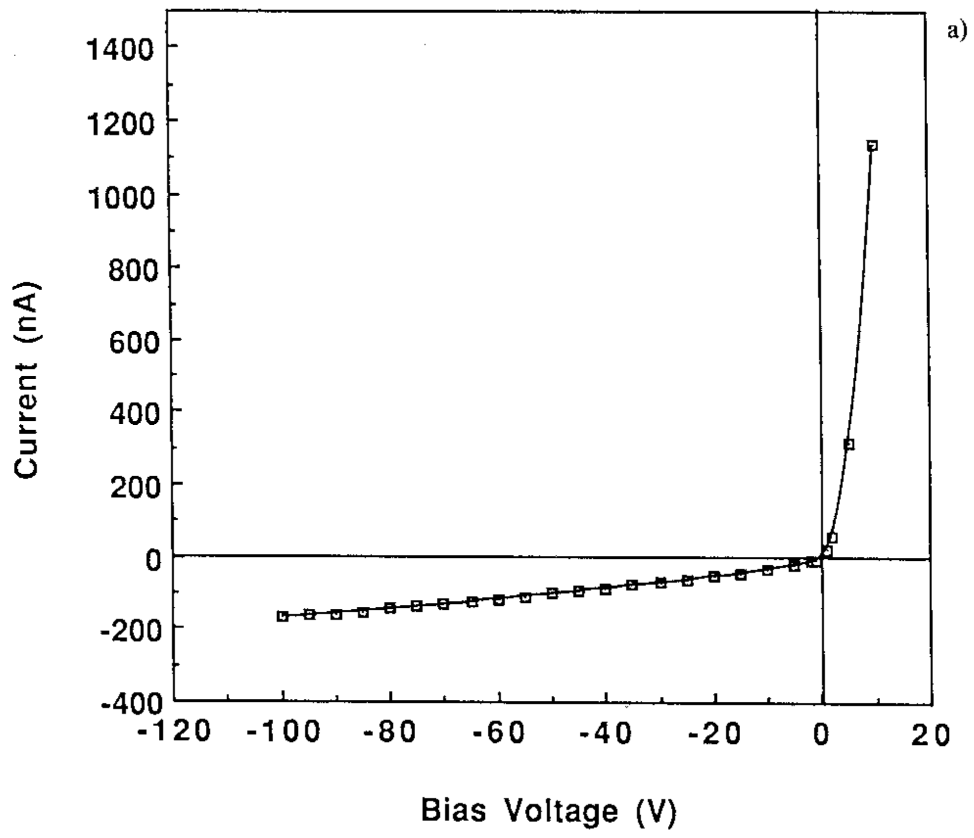

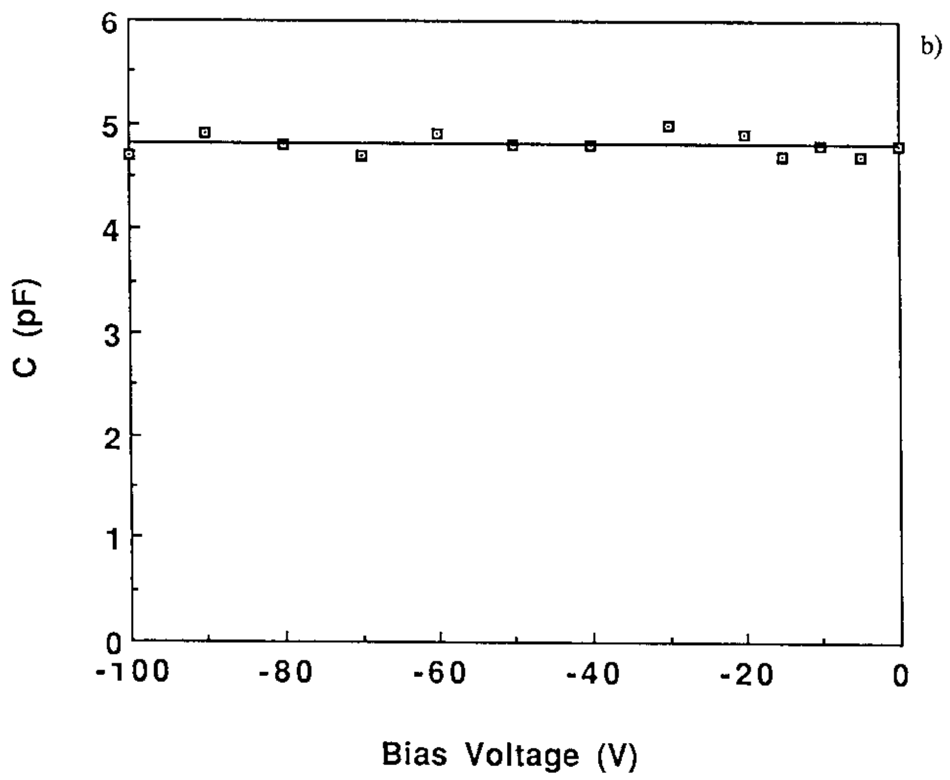

Fig. 1

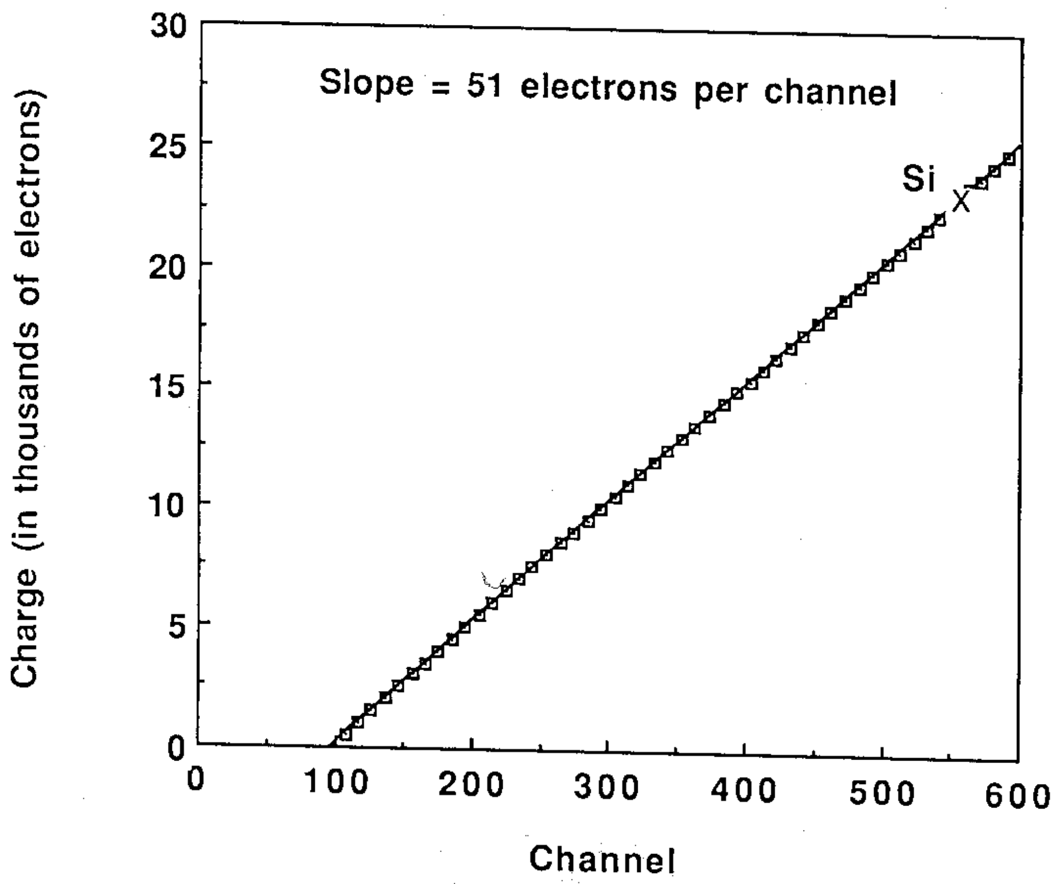

Fig. 2

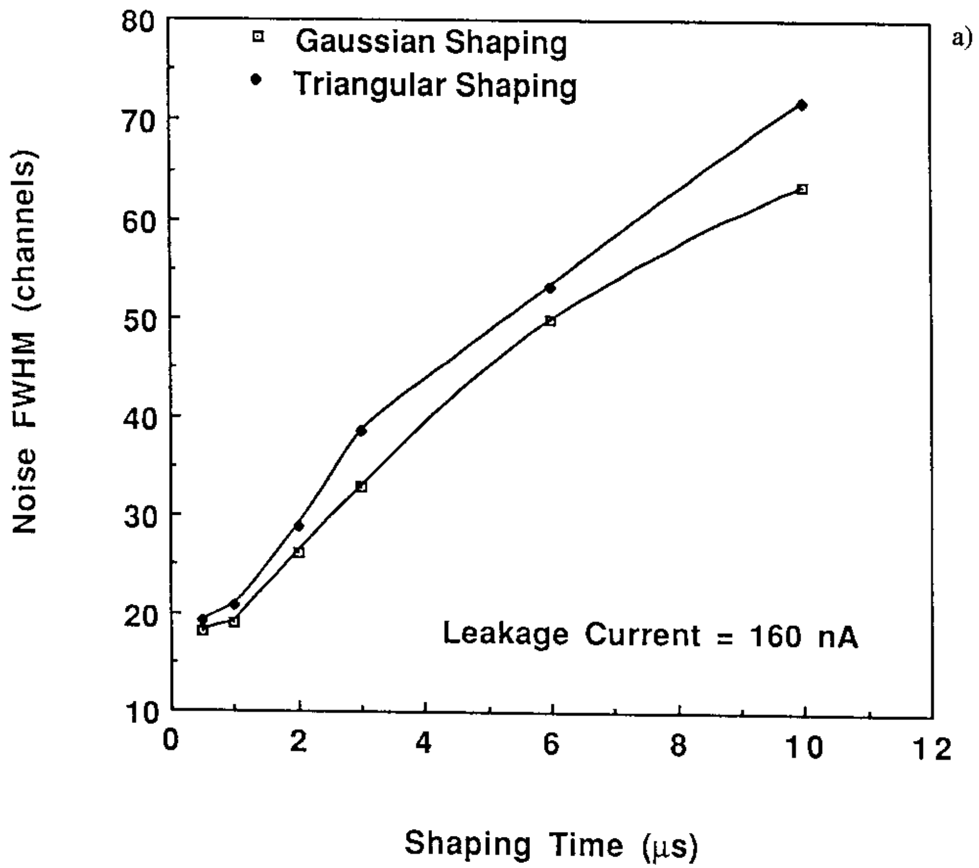

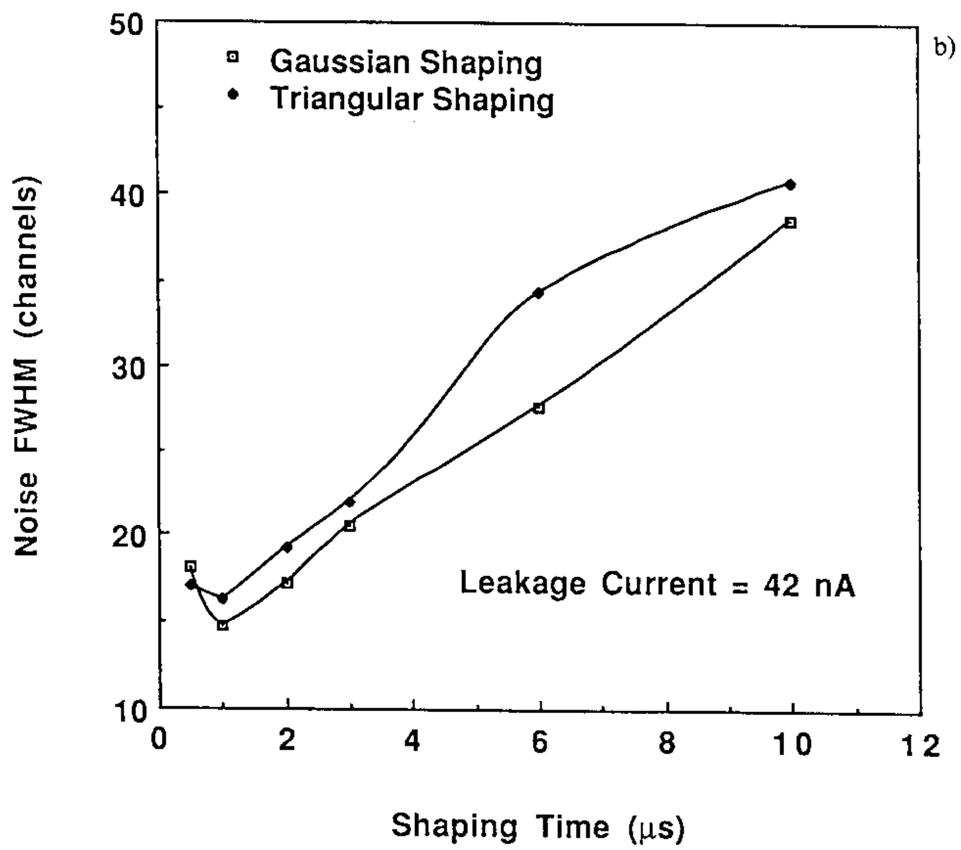

Fig. 3

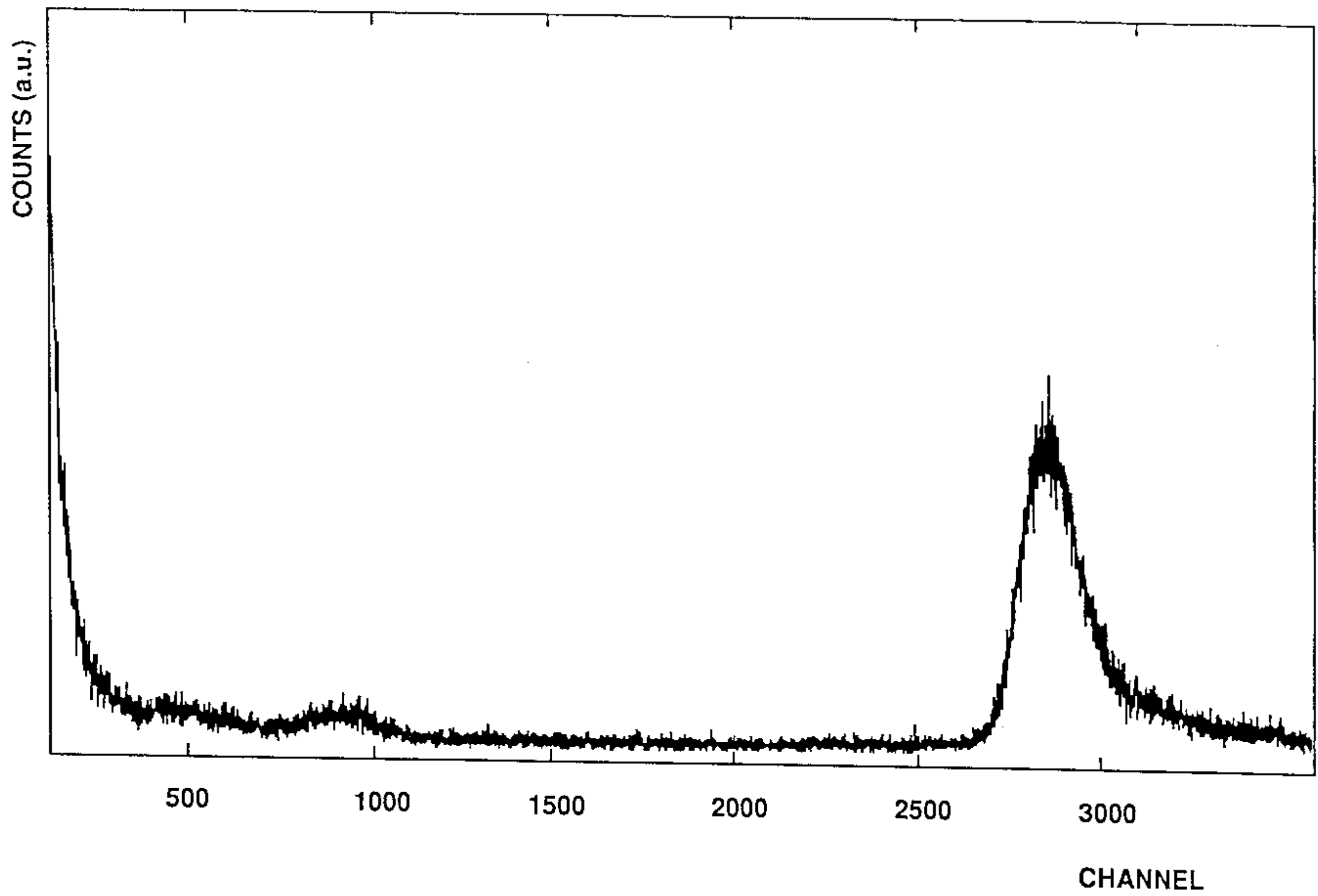

Fig. 4

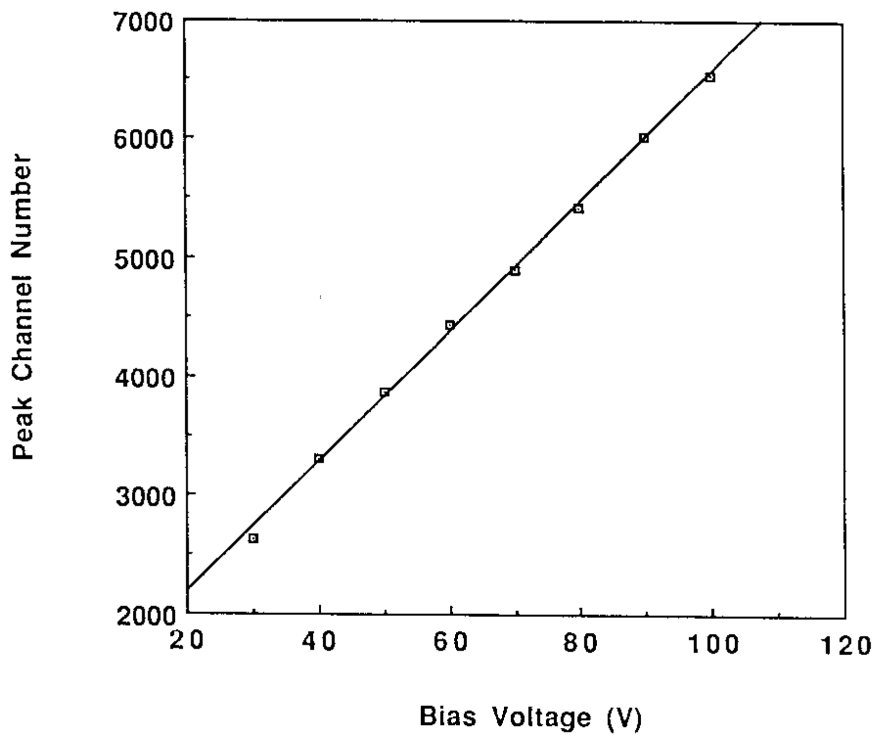

Fig. 5

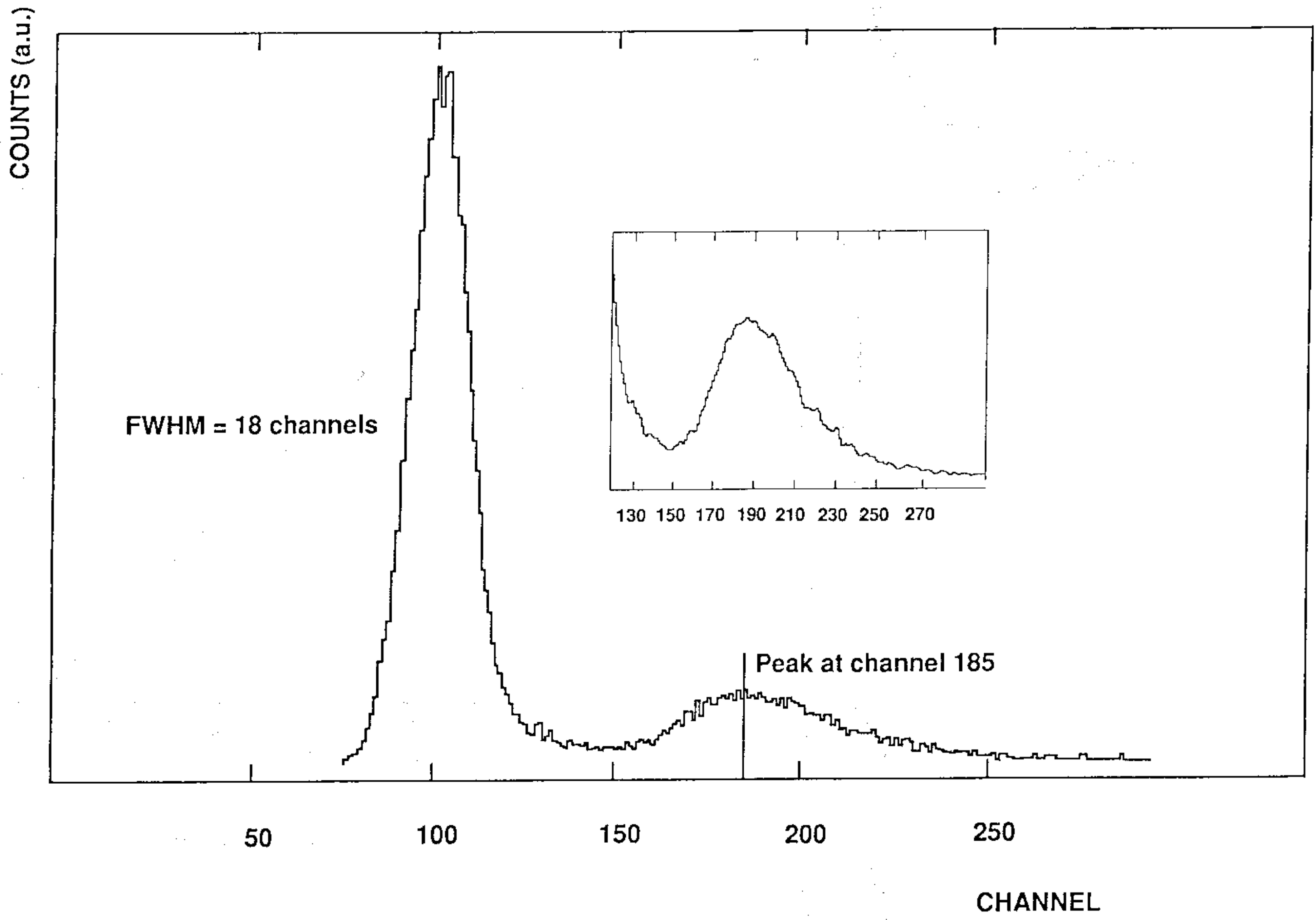

Fig. 6

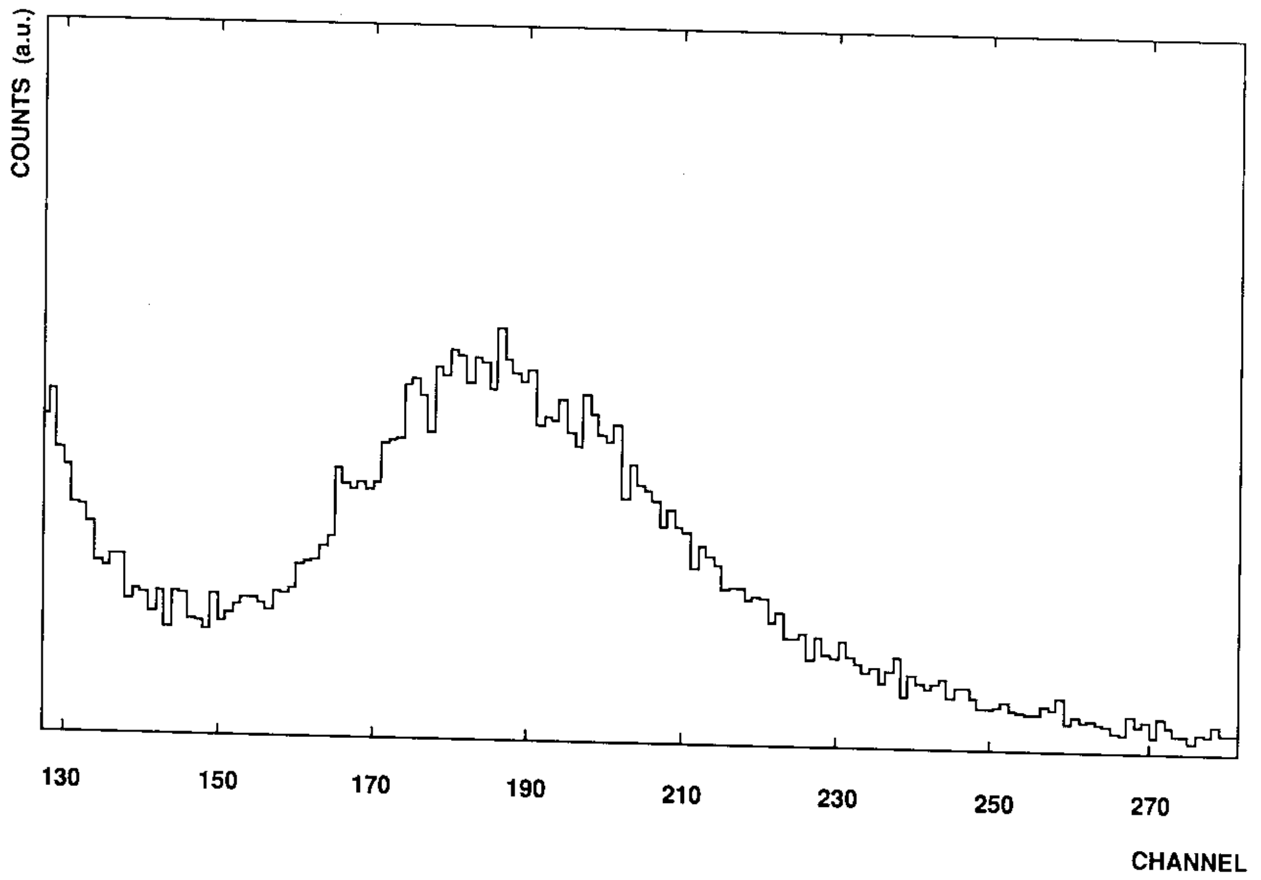

Fig. 7

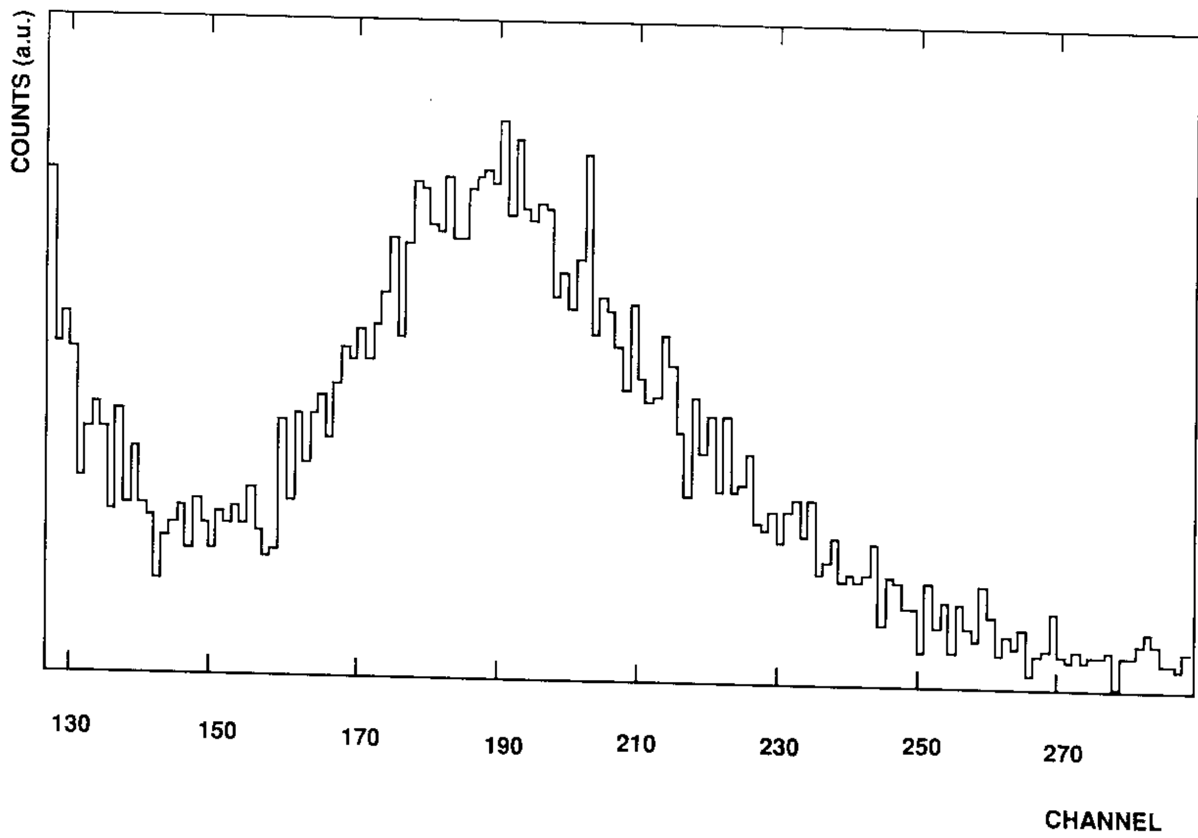

Fig. 8

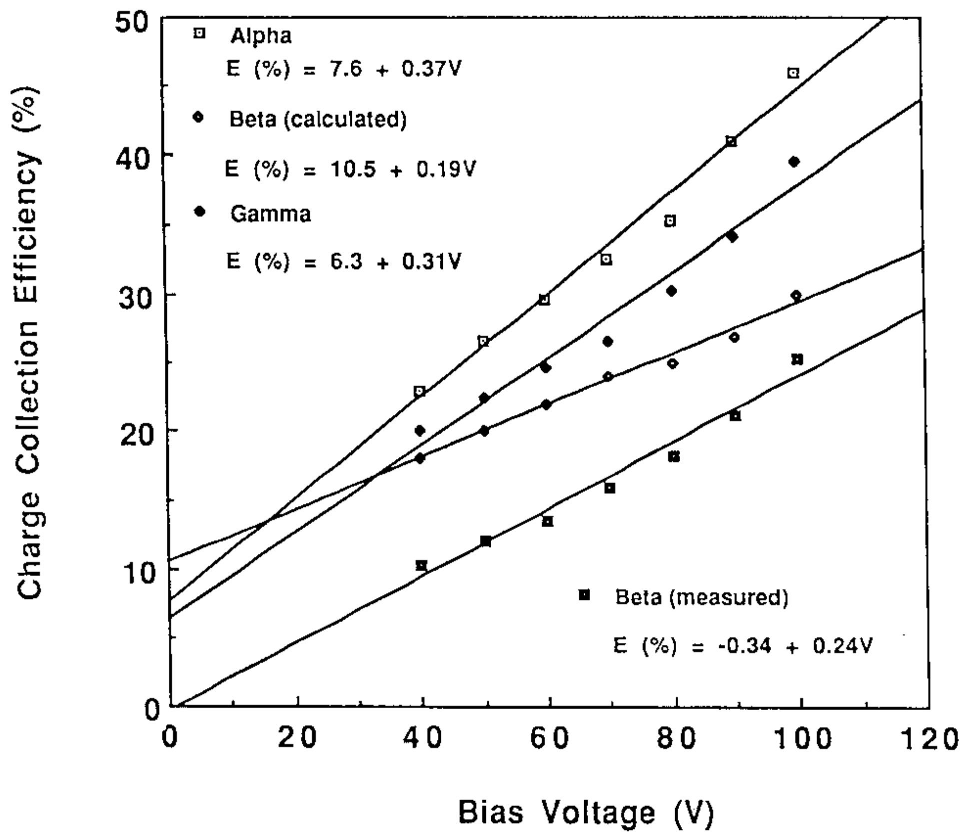

Fig. 9

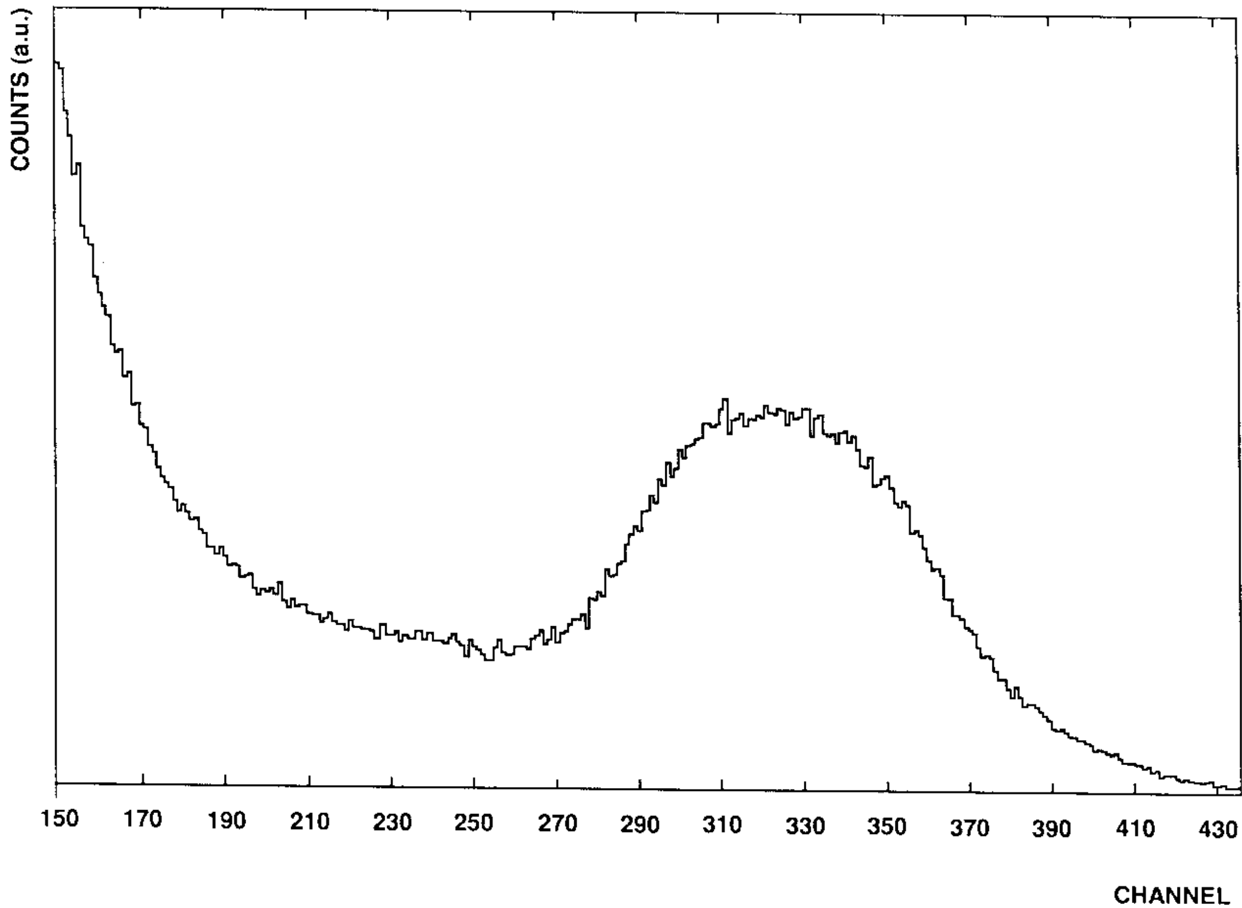

Fig. 10

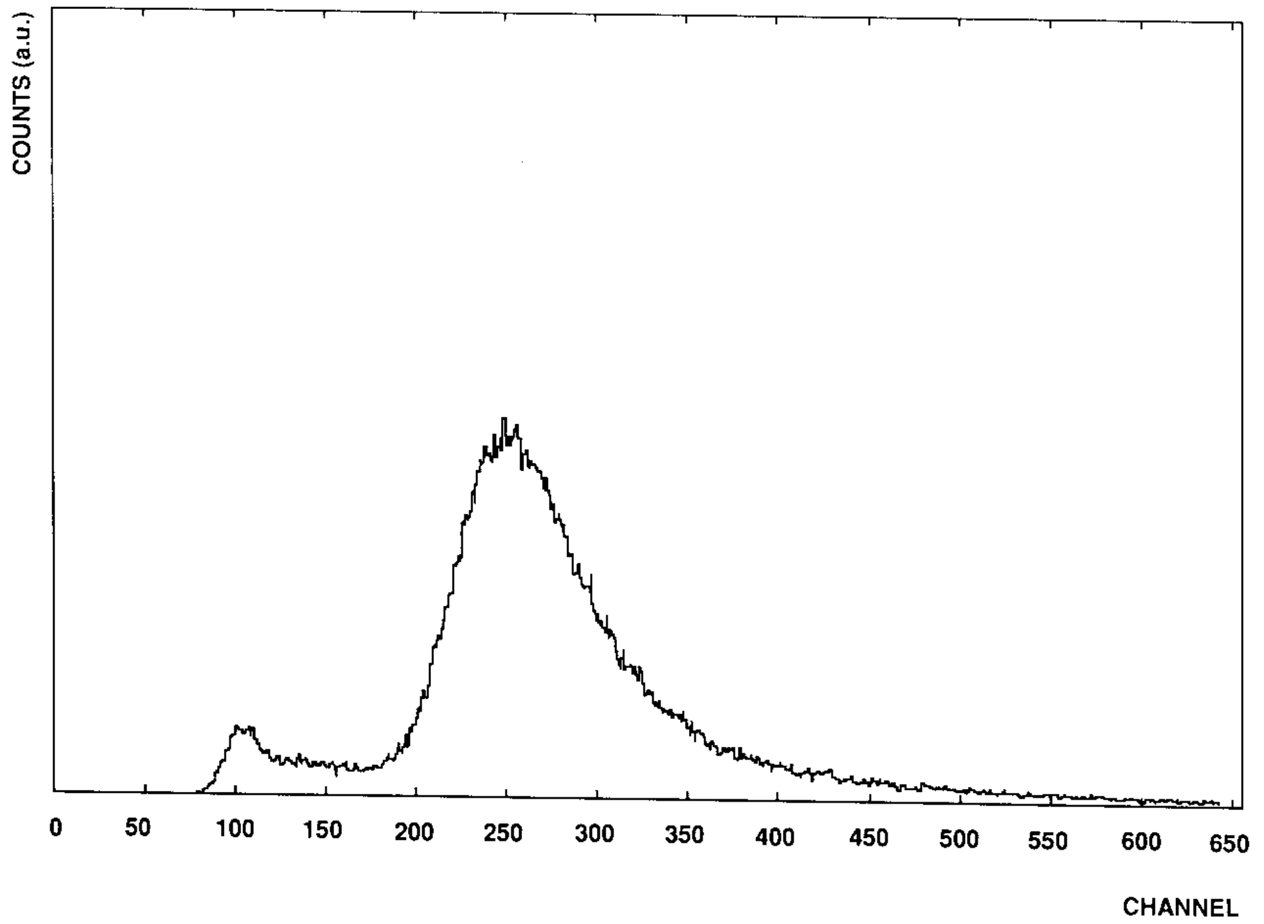

Fig. 11

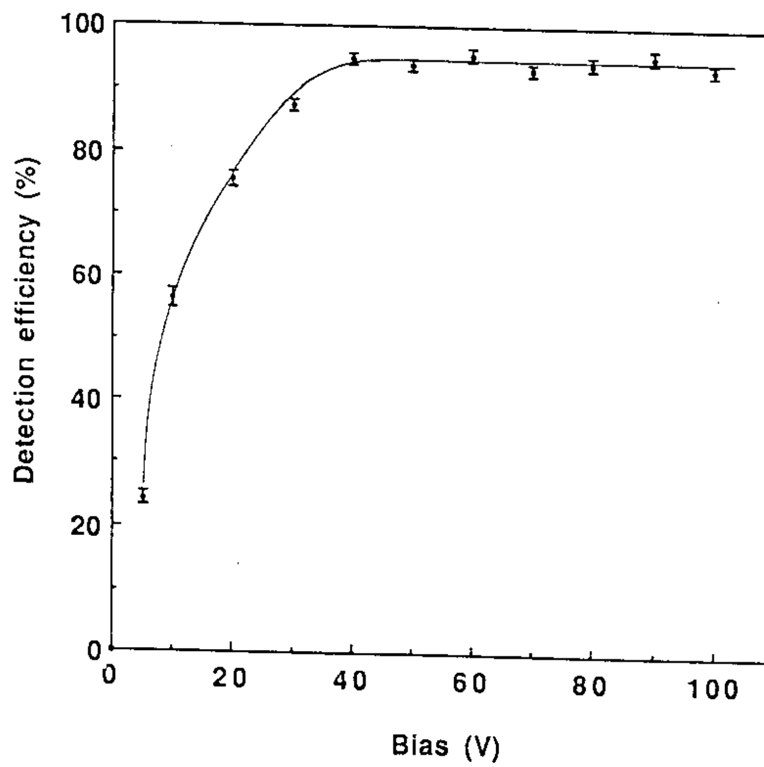

Fig. 12